JOURNAL OF MATERIALS SCIENCE **34** (1999) 1943–1952

Preparation and characterisation of ultrafine lead titanate ($PbTiO_3$) powders

J. FANG[‡], J. WANG[‡*], S. C. NG[§], C. H. CHEW[¶], L. M. GAN[#*]
[‡]*Department of Materials Science,* [§]*Department of Physics,* [¶]*Department of Chemistry and* [#]*Department of Chemistry/IMRE, Faculty of Science, National University of Singapore, Singapore 119260*

Ultrafine lead titanate ($PbTiO_3$) powders in tetragonal form have been successfully prepared via three processing routes, namely, conventional co-precipitation, microemulsion-refined freeze drying, and microemulsion-refined co-precipitation. The formation process of lead titanate from the resulting precursors was monitored using techniques such as thermal analyses and X-ray diffraction for phase identification. It was found that the two microemulsion-refined processing routes led to a lower formation temperature for lead titanate than that observed in the conventional co-precipitation route. The three lead titanate powders have also been compared for particle and agglomerate size distributions and specific surface area. It appears that the microemulsion-refined co-precipitation is the technique which results in the formation of the finest lead titanate powder amongst the three processing routes investigated in the present work.

1. Introduction

Lead titanate ($PbTiO_3$), which exhibits a perovskite structure and a Curie temperature of 490 °C, belongs to the most important ferroelectric and piezoelectric families [1]. It has many important technological applications in electronics and microelectronics, because of its high Curie temperature, high pyroelectric coefficient and high spontaneous polarisation [2, 3]. There are at least two incentives in preparing a ultrafine lead titanate powder, preferably in the range of nanometers: (i) to lower the ferroelectric phase transformation temperature [4]; and (ii) to improve the sintering behaviour of this material [5]. For this, a number of chemistry-based processing routes have been employed, including sol-gel synthesis [6–10], hydrothermal reactions [11–17], co-precipitation [18–25], and emulsion technique [26]. The degree of success of these techniques in preparing a ultrafine lead titanate powder varies considerably from one to another. For example, Lu and Xu was recently successful in synthesising a lead titanate powder of submicrometers in particle size using water-in-oil emulsion [26]. Firstly, they prepared an aqueous solution containing mixed lead nitrate and titanium oxynitrate (Pb : Ti molar ratio = 1 : 1). The aqueous solution was then emulsified in *n*-octane by adding an appropriate amount of surfactant (span 80). Fine lead titanate crystallites in tetragonal form were observed to form in the emulsion-derived precursor when calcined at temperatures above 560 °C.

Microemulsion technique has been successfully used to prepare a range of ultrafine powders, including oxides [27, 28], carbonates [29], silver chloride and bromide [30, 31], high temperature $YBa_2Cu_3O_{7-x}$ superconductor [32, 33], ceramic hydroxyapatite [34] and complex perovskite compounds [35]. There are two types of microemulsion suitable for the process: (i) inverse microemulsion; and (ii) bicontinuous microemulsion. The former is an isotropic dispersion of nanosized aqueous droplets in a continuous oil matrix, stabilised by the presence of an appropriate surfactant. In contrast, the aqueous phase occurs as a continuous three-dimensional channels in the bicontinuous microemulsion. During microemulsion processing, precursor particles are formed in the nanosized aqueous domains, and therefore their sizes are limited in the range of nanometers. It is one of the few techniques which are able to deliver a particle size in the range of nanometers [31, 34, 35].

Conventional powder processing, such as the temperature-assisted reaction of mixed oxides, often results in an unsatisfactory compositional homogeneity in the system with complex perovskite structure. In contrast, a much more homogeneous powder system may be produced via the microemulsion processing route, as has been demonstrated for $LaNiO_3$, La_2CuO_4 and $BaPbO_3$ by Gan *et al.* [36] and for $BaTiO_3$, $BaZrO_3$, $SrTiO_3$ and $SrZrO_3$ by Herrig and Hempelmann [37]. The objectives of the present work are two-fold: (i) to investigate the feasibility of preparing a ultrafine lead titanate powder via microemulsion-based processing routes (microemulsion-refined freeze drying and microemulsion-refined co-precipitation, respectively); and (ii) to characterise the microemulsion-derived lead titanate powder by comparison with that

* Author to whom all correspondence should be addressed.

prepared via a conventional co-precipitation processing route.

2. Experimental procedures

2.1. Starting materials

The starting materials used in the present investigation included lead (II) nitrate (>99.7% in purity, J. T. Baker Inc., USA), titanium (IV) chloride (>99.0% in purity, Hayashi Pure Chemical Industries Ltd., Japan), ammonia solution (concentration: 28.0–30.0 wt %, J. T. Baker Inc., USA), high purity nitric acid (Hetalab Chemical Corporation, USA), high purity cyclohexane (Ajax Chemicals, Australia) and mixed poly (oxyethylene)$_5$ nonyl phenol ether (NP5) and poly (oxyethylene)$_9$ nonyl phenol ether (NP9) (in weight ratio: 2 : 1, Albright and Wilson Asia Pte Ltd., Singapore).

2.2. Preparation of aqueous solution containing 0.30 M [$TiO(NO_3)_2$-$Pb(NO_3)_2$]

Aqueous solution of titanium oxynitrate was prepared by following the procedures of Yamamura *et al.* [38, 39]. Weighed titanium tetrachloride ($TiCl_4$) was dissolved in an appropriate amount of de-ionised water at ice-bath temperature. Cold ammonia solution (12 wt %) was then added into the solution, resulting in the formation of titanium hydroxide hydrate. The gelatinous precipitates were filtered and washed repeatedly using de-ionised water until the pH of filtrate was close to 7.0, in order to remove chloride ions. Titanium oxynitrate in aqueous solution was prepared by dissolving the white precipitates in an appropriate amount of 3.0 M HNO_3, immediately followed by the concentration determination of Ti^{4+} using ICP (Inductively Coupled Plasma, Thermo Jarrell Ash, IRIS/AP). The concentration of $TiO(NO_3)_2$ was then adjusted to 0.30 M by adding an appropriate amount of de-ionised water. To prepare the aqueous solution containing 0.30 M [$Pb(NO_3)_2$-$TiO(NO_3)_2$] at equimolar ratio of Pb^{2+}/Ti^{4+}, an appropriate amount of lead nitrate was dissolved into the aqueous solution of titanium oxynitrate.

2.3. Phase diagrams

The procedure for establishing a partial phase diagram at room temperature for the ternary system consisting of cyclohexane, NP5+NP9 and an aqueous solution containing 0.30 M [$Pb(NO_3)_2$-$TiO(NO_3)_2$] has been detailed elsewhere [36, 40]. To locate the demarcation between the microemulsion (transparent) and non-microemulsion (turbid) regions, the aqueous phase was titrated into a mixture of given cyclohexane to surfactant ratio. Thorough mixing of the three components was achieved using a Vortex mixer. Microemulsion compositions appear optical transparent when the size of aqueous droplets is in the range of 5 to 20 nm, due to the fact that the nanosized aqueous droplets do not cause a substantial degree of light scattering. A series of such demarcation points (transition from transparent to turbid) were obtained by varying the weight ratio of cyclohexane to surfactant. Similarly, a partial phase diagram for the ternary system consisting of cyclohexane, NP5+NP9 and 2.85 M ammonia aqueous solution was constructed by following the same procedure.

2.4. Preparation of $PbTiO_3$ powders

Fig. 1 is a flow chart showing the steps involved in preparing $PbTiO_3$ powders via the three processing routes, namely conventional co-precipitation, microemulsion-refined freeze drying and microemulsion-refined co-precipitation. These three processing routes will be referred to as CPC, MFD and MCP, respectively, in the following discussions.

In the CPC route, an aqueous solution containing 0.30 M [$Pb(NO_3)_2$-$TiO(NO_3)_2$] was titrated at a rate of a few drops per minute into a 12 wt % ammonia solution in a beaker while being vigorously agitated using a mechanical stirrer. The precipitates were recovered by centrifugation and washed repeatedly using de-ionised water, followed by drying at 140 °C in an oven. In the MFD route, a microemulsion consisting of 56.0 wt % cyclohexane, 24.0 wt % NP5+NP9 and 20.0 wt % aqueous phase containing 0.30 M [$Pb(NO_3)_2$-$TiO(NO_3)_2$] was first prepared and kept for one hour at room temperature. The optical transparent mixture was rapidly frozen in a plastic beaker using liquid nitrogen, prior to the freeze-drying in a 1.0 litre freeze dryer (∼−55 °C, 0.01–0.1 mmHg, Benchtop 77400, Labconco) for 90 hours. In the MCP route, two microemulsion systems consisting of two common components, i.e. 56.0 wt % cyclohexane and 24.0 wt % NP5+NP9 and differing only in aqueous phase, were prepared. The aqueous phase for one of the systems was 20.0 wt % of 0.30 M [$Pb(NO_3)_2$-$TiO(NO_3)_2$], while 20.0 wt % of 2.85 M ammonia solution for the other. They were then mixed together by vigorously stirring for more than 20 min. The resulting precursor was retrieved by washing away the oil and surfactant using distilled ethanol, followed by centrifugal recovery and dried at 140 °C for 12 hours.

2.5. Powder characterisations

The as-dried precursors were characterised using thermogravimetric analysis (TGA) and differential thermal analysis (DTA) (Dupont Instruments) at a heating rate of 10 °C/min in air from room temperature up to 900 °C. They were also calcined in air at various temperatures, up to 800 °C, for 1 hour, followed by phase analysis using X-ray diffraction (CuK_α, Philips PW1729). The calcined powders were characterised for particle/agglomerate size distribution using laser scattering technique (Horiba LA-910). BET surface analyser (Nova 2000, Quantachrome) and scanning electron microscope (JEOL, JSM-35CF) were employed to analyse the specific surface area and particle/agglomerate morphology, respectively.

3. Results and discussion

Fig. 2a shows the partial phase diagram established at room temperature for the ternary system consisting of cyclohexane, NP5/NP9 and aqueous solution containing 0.30 M [$Pb(NO_3)_2$-$TiO(NO_3)_2$]. The microemulsion region, which is marked as shaded area in the diagram, widens significantly with increasing NP5+NP9 to cyclohexane ratio. For a given NP5+NP9 to cyclohexane ratio, the microemulsion region is much

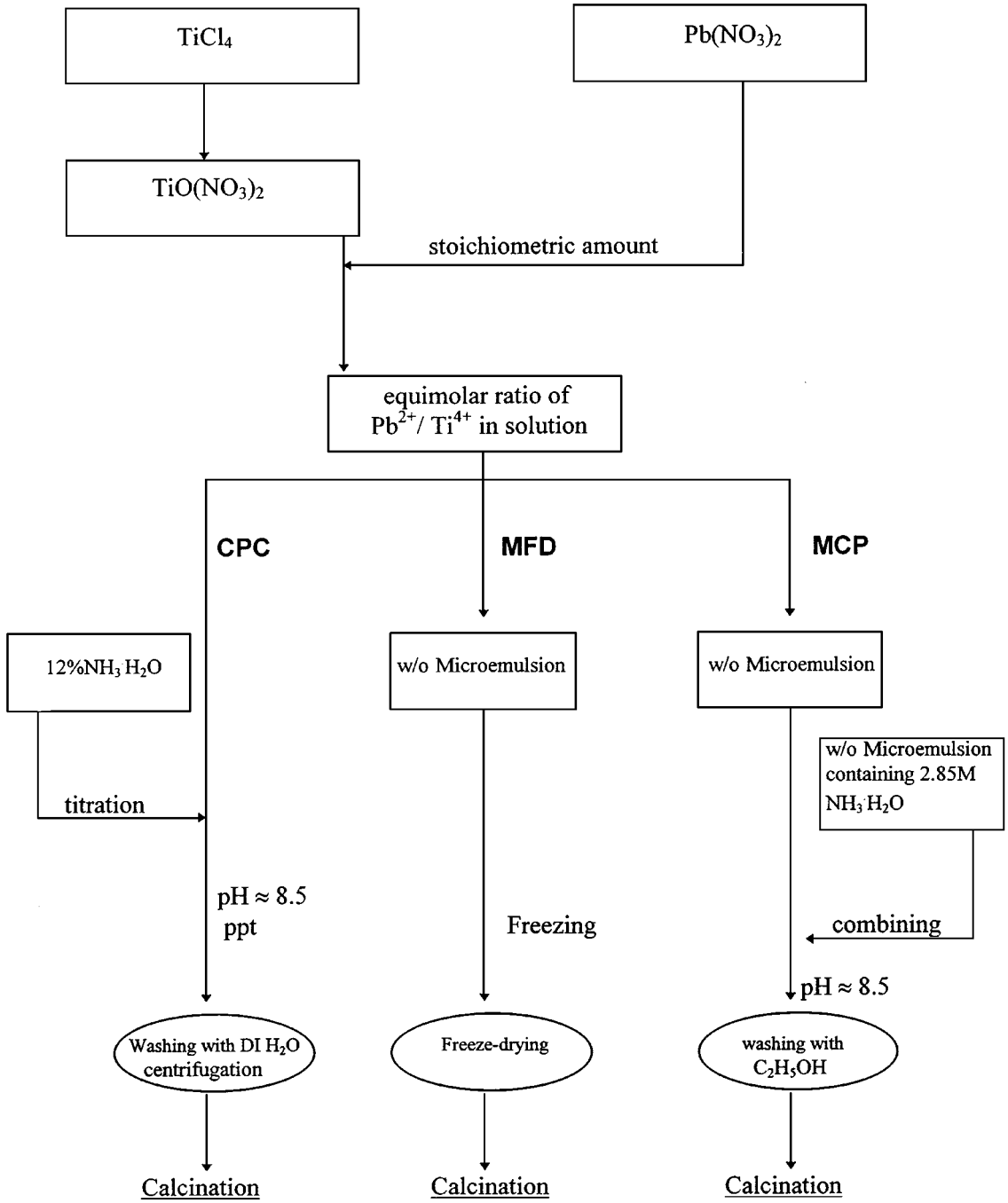

Figure 1 Flow chart for the preparation of $PbTiO_3$ powders via three processing routes.

wider than those observed in the ternary systems containing $ZrO(NO_3)_2$, $Zn(NO_3)_2$ and $Fe(NO_3)_3$ aqueous solutions, respectively [40]. For example, the weight fraction of 0.30 M [$Pb(NO_3)_2$-$TiO(NO_3)_2$] aqueous solution in microemulsion may be increased to ~60% at a NP5+NP9 to cyclohexane ratio of 70 : 30. This offers an apparent advantage of producing a large amount of $PbTiO_3$ powder at the cost of a small amount of oil and surfactant phases. Fig. 2b is the partial phase diagram established at room temperature for the ternary system consisting of cyclohexane, NP5/NP9 and 2.85 M ammonia solution. The microemulsion region also widens with increasing NP5+NP9 to cyclohexane ratio, but not as signficant as for the ternary system containing 0.30 M [$Pb(NO_3)_2$-$TiO(NO_3)_2$] aqueous phase. In general, the maximum loading of 2.85 M ammonia solution in the microemulsion is approximately half that of 0.30 M [$Pb(NO_3)_2$-$TiO(NO_3)_2$]. The compositions consisting of 56.0 wt % cyclohexane, 24.0 wt % NP5+NP9 and 20.0 wt % aqueous phase containing 0.30 M [$Pb(NO_3)_2$-$TiO(NO_3)_2$] and 2.85 M ammonia solutions, respectively, were chosen for the preparation of $PbTiO_3$ powders in the MFD and MCP routes. Both of the microemulsion composition points are marked by "×" as shown in Figs 2a and 2b.

Figs 3a, b and c are the TGA curves of lead titanate precursors prepared via the three processing routes, respectively. In correlating the TGA results, Figs 4a, b and c show the DTA curves of the three powder precursors, respectively. The precursor prepared via the CPC route demonstrates a two-stage weight loss, a steady weight loss over the temperature range from room temperature to 350 °C and a sharp fall in specimen weight over the temperature range from 400 to 490 °C. Little

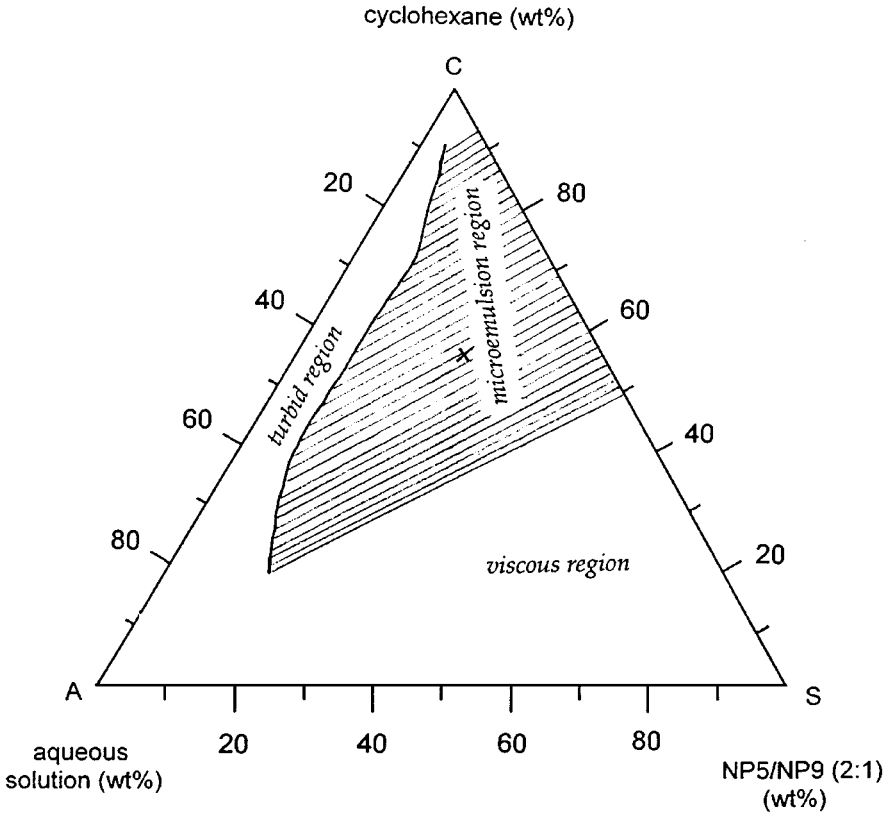

(a)

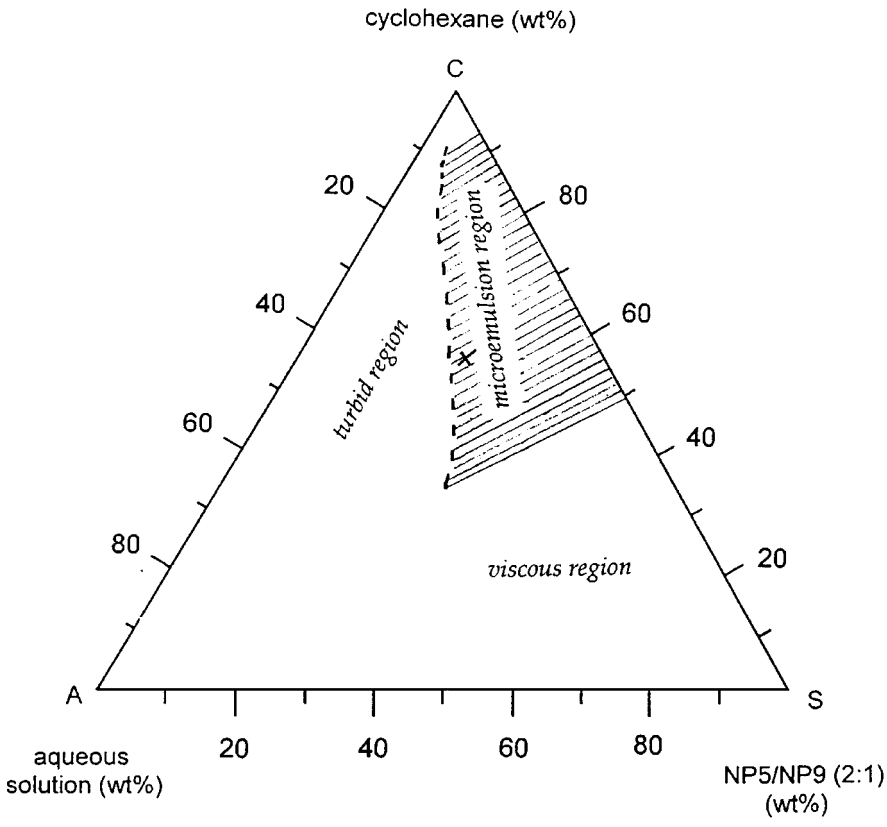

(b)

Figure 2 (a) Partial phase diagram established at room temperature for the ternary system consisting of cyclohexane, NP5+NP9, and aqueous solution containing 0.30 M [$Pb(NO_3)_2$-$TiO(NO_3)_2$]. (b) Partial phase diagram established at room temperature for the ternary system consisting of cyclohexane, NP5+NP9 and 2.85 M ammonia solution.

further weight loss is observed at temperatures above 500 °C, indicating the completion of all the reactions involving a weight loss. The weight loss at temperatures below 350 °C is believed to be due to the elimination of residual water and the dehydration of hydroxide hydrates in the precursor [14, 41]. The fall in specimen weight over the temperature range from 400 to 490 °C is related to the decomposition of lead hydroxide as well

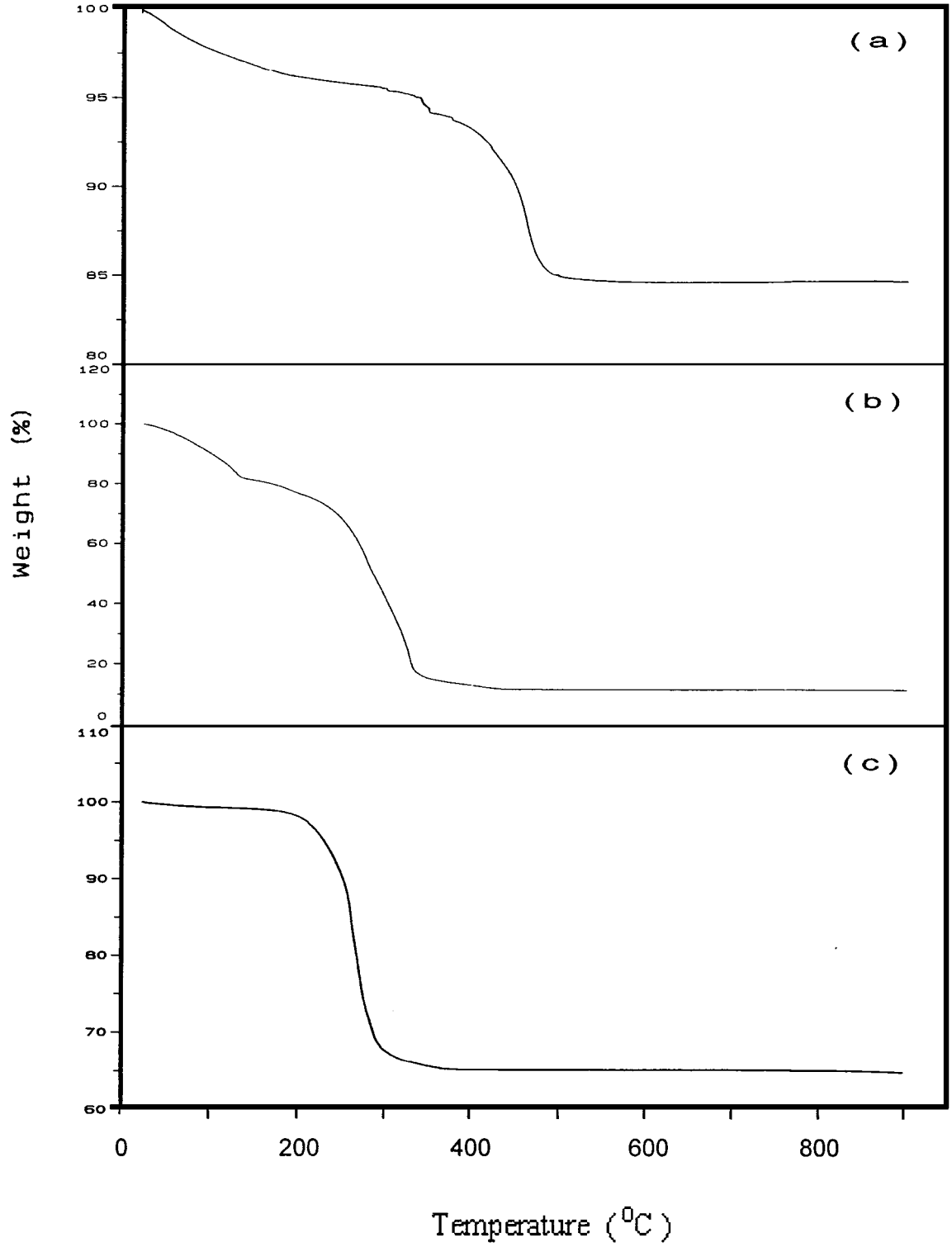

Figure 3 TGA traces for the precursors prepared via (a) conventional co-precipitation; (b) microemulsion-refined freeze drying; and (c) microemulsion-refined co-precipitation.

as titanyl hydroxides and the formation of lead titanate. As shown in Fig. 4a, this corresponds to an endothermic reaction over the same temperature range in DTA trace of the precursor. The precursor prepared via the MFD route also exhibits a steady weight loss from room temperature to 150 °C and the weight loss slows down over the temperature range from 150 to 230 °C. There is then a fall in specimen weight over the temperature range from 250 to 340 °C. No further weight loss is observed with increasing temperature for the precursor at temperatures above 350 °C. The elimination of residual oil and surfactant phases and water is responsible for the steady weight loss at temperatures below 230 °C. The fall in specimen weight over the temperature range from 250 to 340 °C is believed to be due to the decomposition of lead and titanium nitrates/oxynitrates and the formation of lead and titanium oxides [41]. This is supported by a large exothermic peak occurring over the temperature range from 330 to 390 °C. Fig. 4b shows that there is another large exothermic peak over the temperature range from 420 to 500 °C for the precursor. As will be discussed later, it is related to the formation of

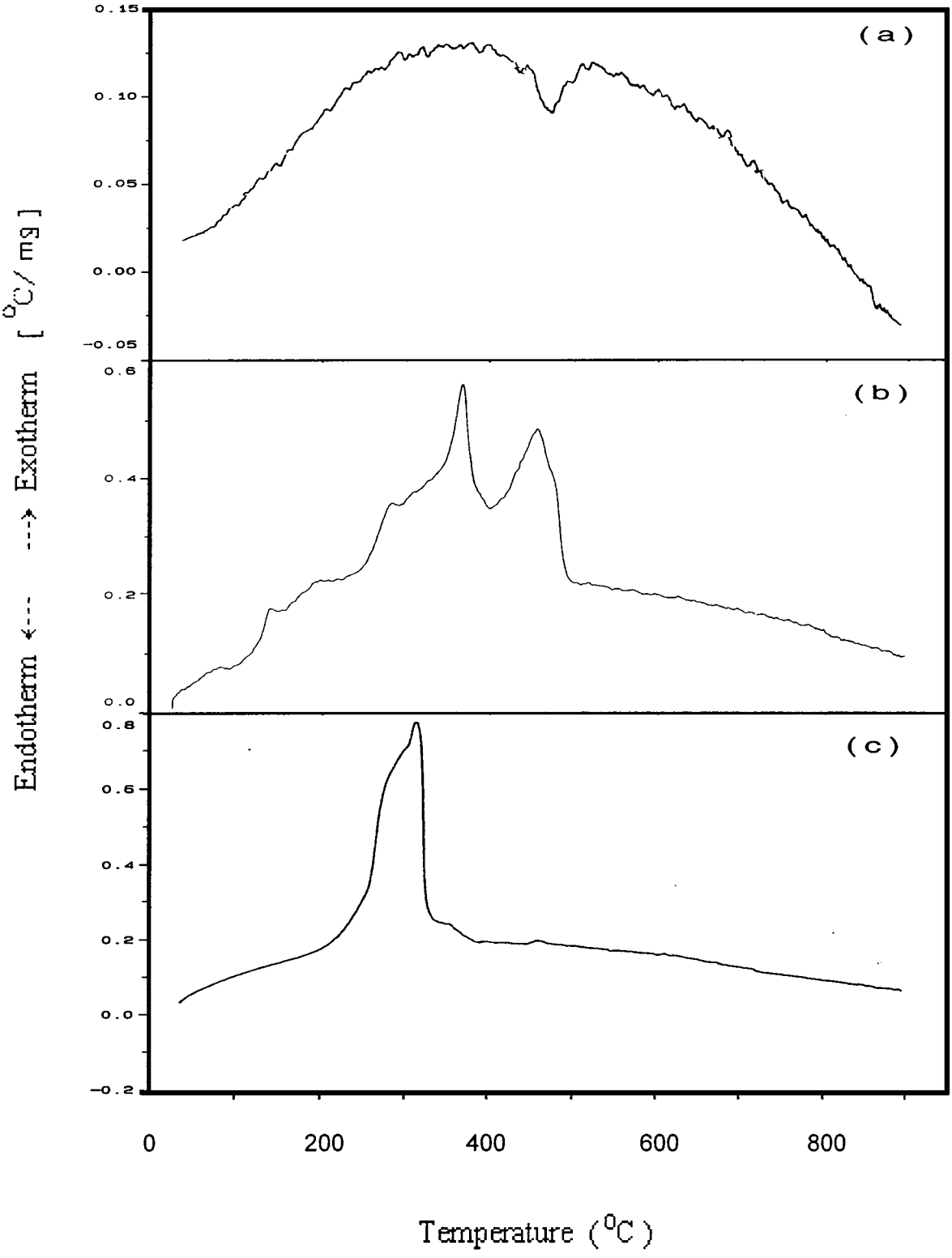

Figure 4 DTA traces for the precursors prepared via (a) conventional co-precipitation; (b) microemulsion-refined freeze drying; and (c) microemulsion-refined co-precipitation.

lead titanate as a result of the reaction between lead oxide and titanium oxide.

Fig. 3c shows that the precursor prepared via the MCP route exhibits little weight loss over the temperature range from room temperature to 200 °C. However, there is a significant weight loss occurring over the temperature range from 230 to 320 °C. As shown in Fig. 4c, there is a large exothermic reaction over the same temperature range. This is apparently due to the decomposition of lead and titanium hydroxide hydrates, together with the elimination of residual oil and surfactant phases from the precursor.

To study the phase development with increasing calcination temperature in each of the three precursors, they were calcined for 1 hour in air at various temperatures, up to 800 °C, followed by phase analysis using XRD. Figs 5 to 7 are the XRD traces at various calcination temperatures for the precursors prepared via the CPC, MFD and MCP routes, respectively. Fine $PbTiO_3$ crystallites were developed in the co-precipitated

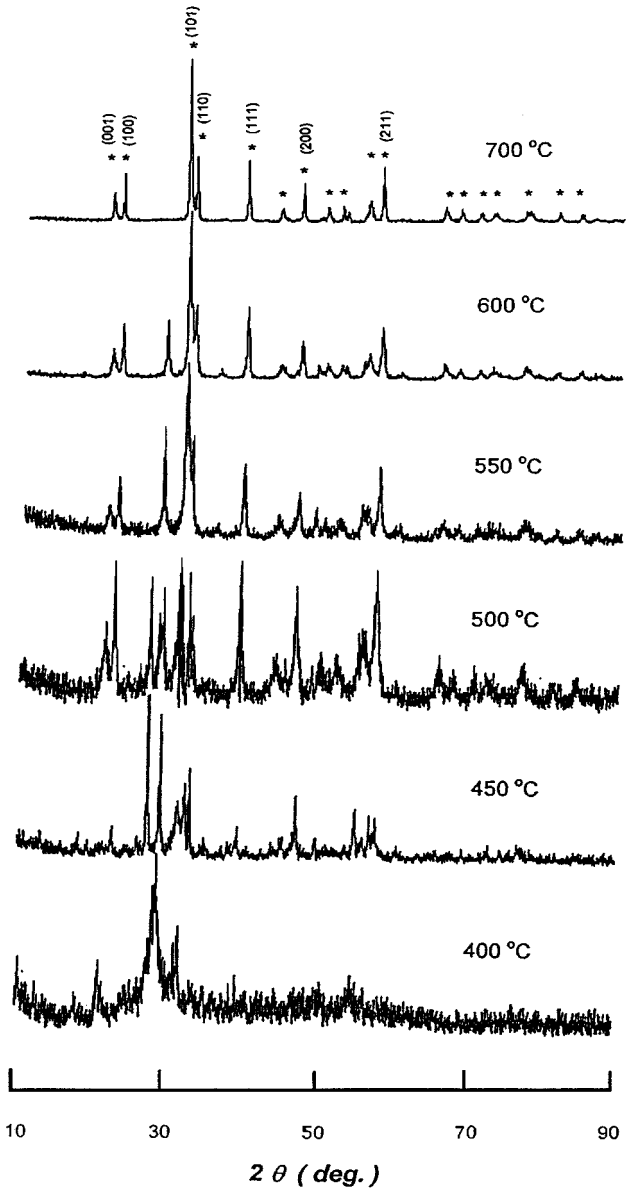

Figure 5 XRD traces of the co-precipitated $PbTiO_3$ powders, calcined for 1 hour at 400, 450, 500, 550, 600 and 700 °C, respectively.

precursor when it was calcined at 400 °C. With increasing calcination temperature from 400 to 550 °C, the amount of $PbTiO_3$ phase increased at the expenses of non-$PbTiO_3$ phases. However, a high purity $PbTiO_3$ powder is obtainable only when the precursor is calcined at temperatures above 700 °C.

The precursor prepared via the MFD route consists of crystalline lead oxide and titanium oxide when calcined at 400 °C. This is consistent with the results of TGA and DTA study. As discussed above, the precursor did not show any further significant weight loss at temperatures above 400 °C and it exhibited a large exothermic peak over the temperature range from 330 to 390 °C, indicating the formation of these oxides. It contains a large percentage of tetragonal $PbTiO_3$ phase when calcined at 450 °C and tetragonal $PbTiO_3$ becomes the predominant phase in the precursor at 500 °C. This suggests that the exothermic reaction over the temperature range from 420 to 500 °C (Fig. 4b) is due to the formation of $PbTiO_3$ as a result of the reaction between lead oxide and titanium oxide. Calcination over the temperature range from 500 to 600 °C results in a steady elimination of non-$PbTiO_3$ phases. Tetragonal $PbTiO_3$ is the only detectable phase using XRD when the precursor is calcined at 650 °C for 1 hour.

As shown in Fig. 7, fine $PbTiO_3$ crystallites are developed in the MCP precursor at a calcination temperature of as low as 350 °C and tetragonal $PbTiO_3$ becomes a predominant phase at 450 °C. Crystalline tetragonal $PbTiO_3$ is the only detectable phase in the precursor when it is calcined at 500 °C. Therefore, the precursor has the lowest formation temperature for tetragonal $PbTiO_3$ amongst the precursors prepared via the three processing routes investigated in the present work. It is lower than those reported for the precursors prepared via many other chemistry-based processing routes. For example, a calcination temperature of >700 °C was required for the formation of a high purity $PbTiO_3$ in the emulsion-derived precursor, although tetragonal $PbTiO_3$ crystallites were observed to form at 560 °C [26]. A similar calcination temperature was needed for the hydrolysed precursor from alkoxides [4]. The calcination temperature required for the co-precipitated precursors was in the range of 700 to 800 °C [8, 19, 25],

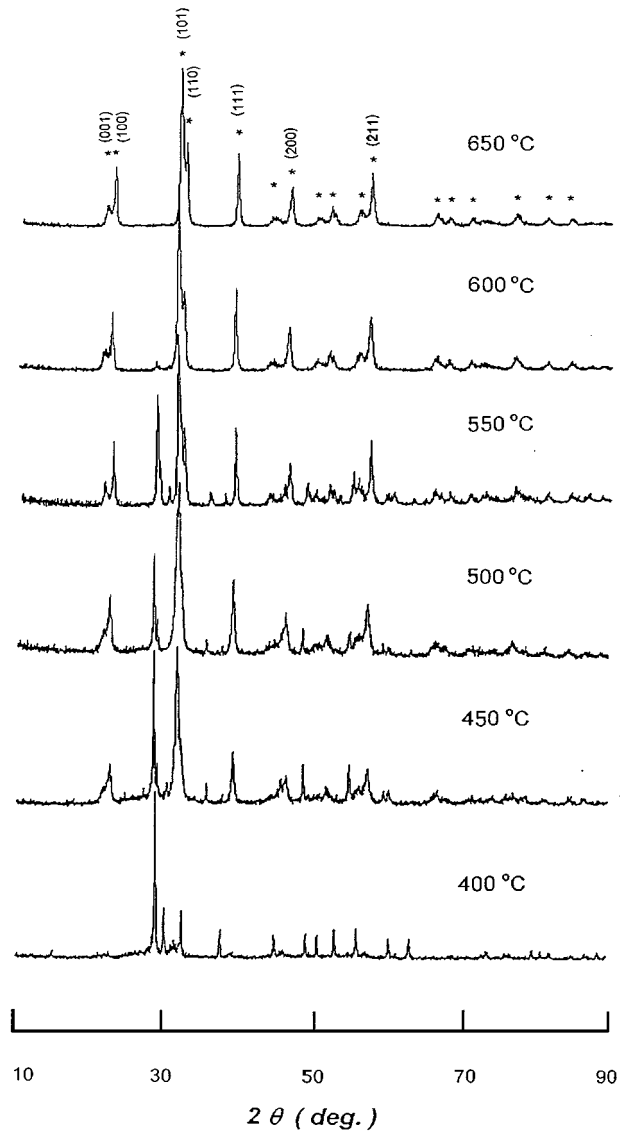

Figure 6 XRD traces of the $PbTiO_3$ powders prepared via the microemulsion-refined freeze drying route and calcined for 1 hour at 400, 450, 500, 550, 600 and 650 °C, respectively.

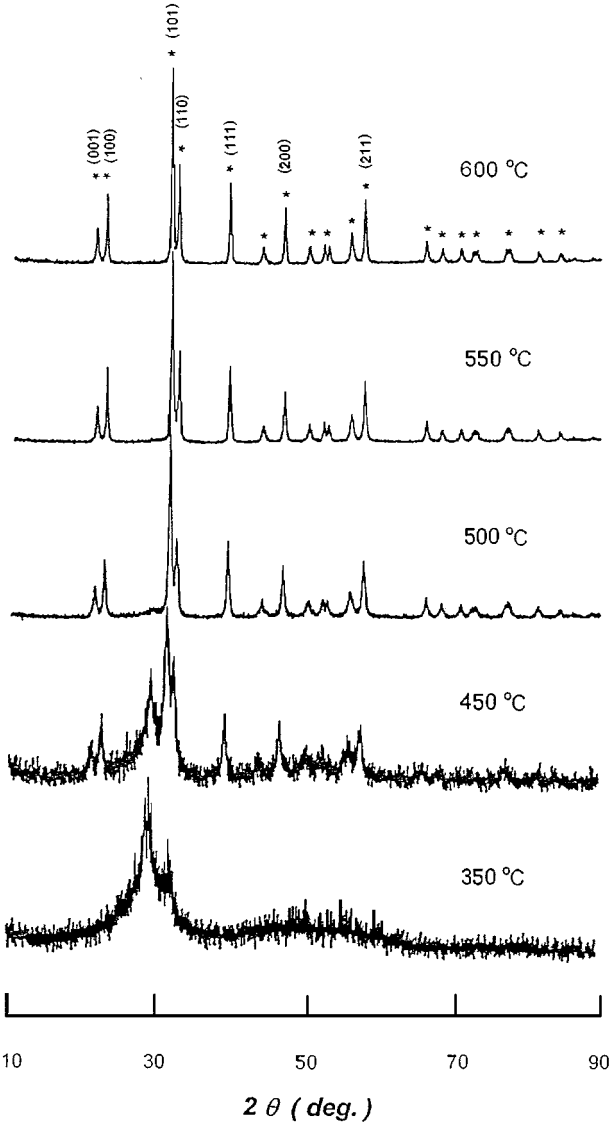

Figure 7 XRD traces of the $PbTiO_3$ powders prepared via the microemulsion-refined co-precipitation route and calcined at for 1 hour at 350, 450, 500, 550 and 600 °C, respectively.

which is very similar to that observed in the CPC precursor.

The $PbTiO_3$ powders prepared via the three processing routes are different in particle/agglomerate size and morphology. Figs 8a, b and c are three SEM micrographs showing the microstructure of the three powders, respectively. They were all calcined at 600 °C for 1 hour. The co-precipitation derived $PbTiO_3$ powder consists of primary particles of 0.1 to 0.2 μm in size. They occur as small aggregates of 0.5 to 1.0 μm in size. The strong inter-particle bond within each aggregate is evidenced by the formation of a well established necking between neighbouring particles. In contrast, primary particles in $PbTiO_3$ powder prepared via the MFD route are smaller than those in the co-precipitated powder, although particle agglomeration has also occurred in the powder. An intermediate primary particle size between the above two is observed for the powder prepared via the MCP route, Fig. 8c. These results of SEM observation are supported by the particle size measurement using BET specific surface analyser. A specific surface area of 6.59, 35.23 and 12.92 m^2/g were measured for the $PbTiO_3$ powders prepared via the CPC, MFD and MCP processing routes, respectively. This corresponds to an average particle size of 0.115, 0.021 and 0.058 μm for the three powders, respectively.

In correlating the above microstructural studies using SEM, Figs 9a, b and c are particle/agglomerate size distributions measured by laser scattering technique for the three $PbTiO_3$ powders, respectively. All these three powders were calcined at 600 °C for 1 hour, followed by a treatment using 5 wt % boiling acetic acid in order to remove lead oxide and pyrochlore phases. Two types of measurement were then carried out for each of these three powders: (i) measurement without ultrasonic dispersion; and (ii) measurement with a 10 min of ultrasonic dispersion. Apparently, the ultrasonication aims to disperse those soft particle agglomerates in the powder. As shown in Fig. 9a, the powder prepared via the CPC route exhibits an average particle/agglomerate size of 0.22 and 0.30 μm, respectively, for the with- and without-ultrasonication measurements. Therefore, the difference between the two measurements is not significant. This is in agreement with the SEM observation that the particle aggregates in this powder are "hard" in nature. The 10 min of ultrasonic dispersion did not result in the disintegration of many of these aggregates. Fig. 9b shows that the particles/agglomerates in the $PbTiO_3$ powder prepared via the MFD route are slightly bigger than those in the powder prepared via the CPC route. The difference between the with-ultrasonication measurement (average size: 0.23 μm) and without-ultrasonication measurement (average size: 0.35 μm) is also slightly bigger than that for the conventionally co-precipitated $PbTiO_3$ powder. But there is a remarkable difference between the with-ultrasonication measurement (average size: 0.11 μm) and the without-ultrasonication measurement (average size: 0.43 μm) for the $PbTiO_3$ powder prepared via the MCP route. Therefore, the particle agglomerates in this powder are soft and dispersible by conventional ultrasonication. This will offer an apparent advantage towards achieving a high sintered density and homogeneous microstructure for lead titanate ceramics at a reduced sintering temperature.

4. Conclusions

Ultrafine lead titanate powders in tetragonal form have been successfully prepared via three processing routes, namely conventional co-precipitation, microemulsion refined freeze drying and microemulsion refined co-precipitation. Precursors derived from these three processing routes exhibit very different formation temperature for tetragonal $PbTiO_3$ phase. The co-precipitated precursor requires a calcination at 700 °C for 1 hour, in order to be developed into a high purity $PbTiO_3$ powder. This is in contrast to 650 °C for 1 hour and 500 °C for 1 hour needed for the precursors derived via the microemulsion refined freeze drying and microemulsion refined co-precipitation routes, respectively. The two microemulsion refined processing routes also result in the formation of finer $PbTiO_3$ powders than that prepared via the conventional co-precipitation route, as observed using SEM and BET surface analyser in the powders calcined at 600 °C for 1 hour. Particle size

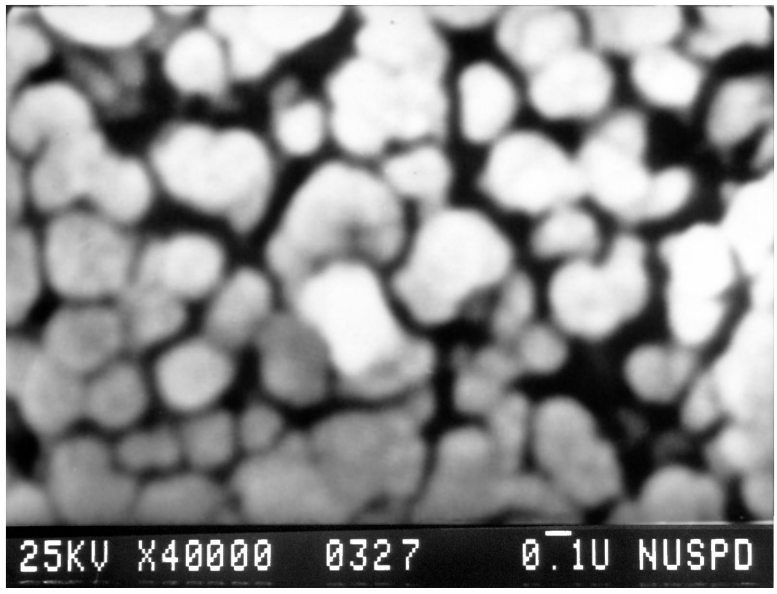

(a)

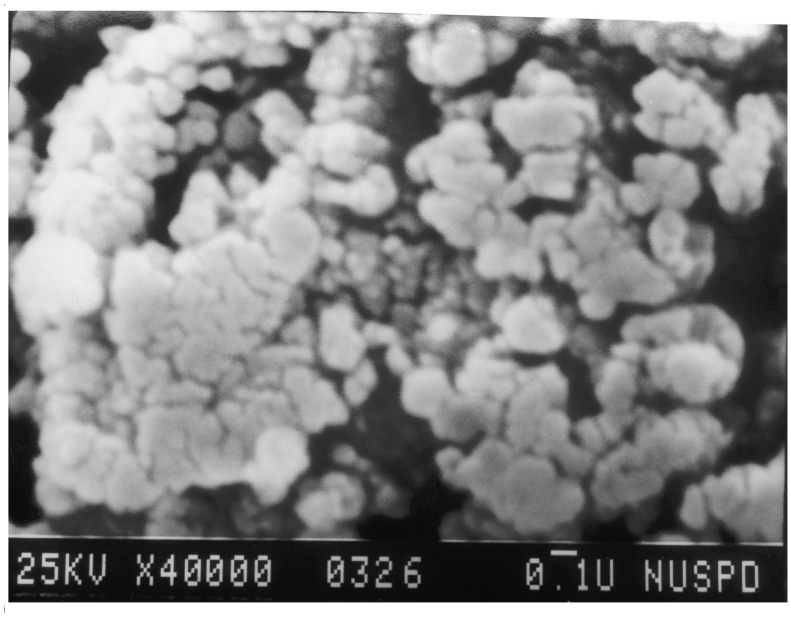

(b)

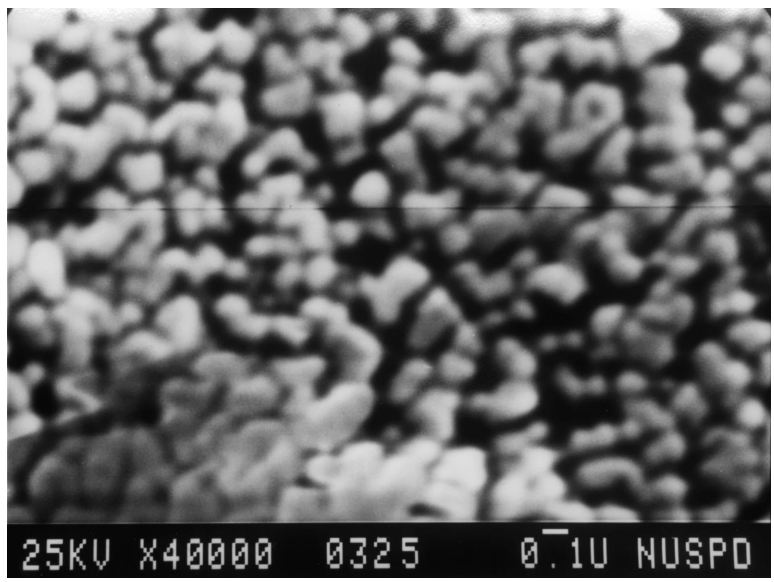

(c)

Figure 8 (a, b, c) SEM micrographs showing the microstructure of $PbTiO_3$ powders prepared via the conventional co-precipitation, micro-emulsion-refined freeze drying and microemulsion-refined co-precipitation, respectively. All the three powders were calcined at 600 °C for 1 hour, followed by treatment in 5 wt % acetic acid.

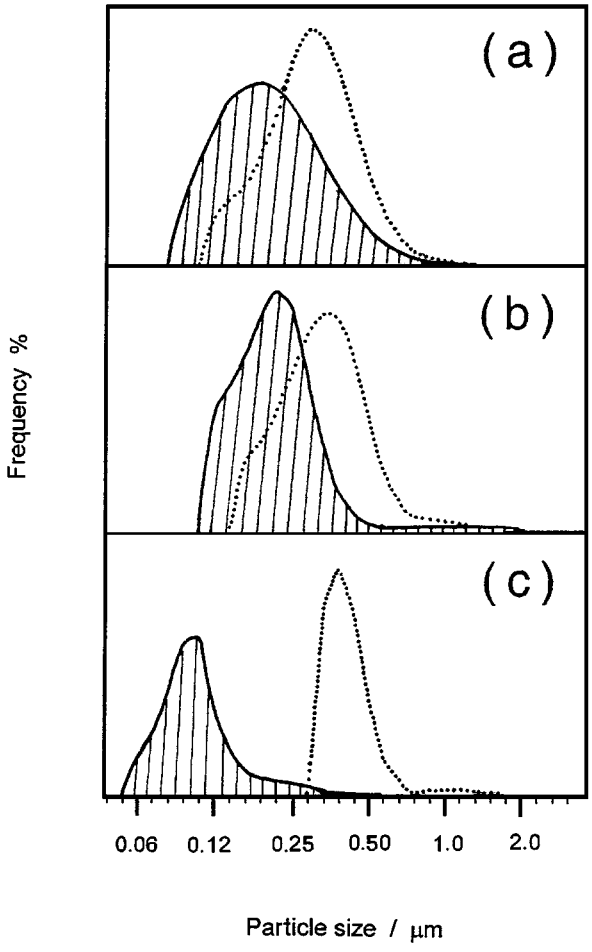

Figure 9 The particle/agglomerate size distributions of $PbTiO_3$ powders prepared via (a) conventional co-precipitation, (b) microemulsion-refined freeze drying, and (c) microemulsion-refined co-precipitation, respectively. Two measurements were made for each of the three powders: without ultrasonication (•••••) and with a 10 min of ultrasonication (—). The powders were calcined at 600 °C for 1 hour.

measurement using laser scattering technique indicates that the $PbTiO_3$ powder prepared via the microemulsion refined co-precipitation route exhibits the smallest agglomerate size amongst the three powders.

Acknowledgements

The authors wish to thank Madam Pang Teng Jar of the Department of Physics at the National University of Singapore for her help in using the X-ray diffractometer. This work was supported by research grants RP950613 and RP950605 from the National University of Singapore.

References

1. C. CHANDLER, C. ROGER and M. HAMPDEN-SMITH, *Chem. Rev.* **93** (1993) 1205.
2. W. C. HENDRICKS, S. B. DESU and C. H. PENG, *Chem. Mater.* **6** (1994) 1955.
3. J. S. WRIGHT and L. F. FRANCIS, *J. Mater. Res.* **8** (1993) 1712.
4. K. ISHIKAWA, N. OKADA, K. TAKADA, T. NOMURA and M. HAGINO, *Jpn. J. Appl. Phys.* **33** (1994) 3495.
5. "Electronic Ceramics," edited by L. M. Levinson (Marcel Dekker Inc., New York, 1988) p. 209.
6. D. BERSANI, P. P. LOTTICI, A. MONTENERO, S. PIGONI and G. GNAPPI, *J. Mater. Sci.* **31** (1996) 3153.
7. L. LAN, A. MONTENERO, G. GNAPPI and E. DRADI, *J. Mater. Res.* **30** (1995) 3137.
8. J. B. BLUM and S. R. GURKOVICH, *ibid.* **20** (1985) 4479.
9. S. R. GURKOVICH and J. B. BLUM, *Ferroelectrics* **62** (1985) 189.
10. P. LÖBMANN, W. GLAUBITT, J. GROSS and J. FRICKE, *J. Non-Cryst. Solids* **186** (1995) 59.
11. C. H. LIN, S. C. PEI, T. S. CHIN and T. P. WU, *Ceram. Trans.* **30** (1993) 261.
12. K. KIKUTA, A. TOSA, T. YOGO and S. HIRANO, *Chem. Lett.* (1994) 2267.
13. H. CHENG, J. MA, Z. ZHAO and L. QI, *J. Mater. Sci. Lett.* **15** (1996) 1245.
14. Y. OHARA, K. KOUMOTO, T. SHIMIZU and H. YANAGIDA, *J. Mater. Sci.* **30** (1995) 263.
15. S. SATO, T. MURAKATA, H. YANAGI and F. MIYASAKA, *ibid.* **29** (1994) 5657.
16. H. CHENG, J. MA, Z. ZHAO, D. QIANG, Y. LI and X. YAO, *J. Amer. Ceram. Soc.* **75** (1992) 1123.
17. S. KANEKO and F. IMOTO, *Bull. Chem. Soc. Jpn.* **51** (1978) 1739.
18. C. M. JIMENEZ, G. F. ARROYO and L. D. O. GUILLEN, in "Ceramic Powders," edited by P. Vincenzini (Elsevier, Amsterdam, 1983) p. 565.
19. G.R. FOX, E. BREVAL and R.E. NEWNHAM, *J. Mater. Sci.* **26** (1991) 2566.
20. G. R. FOX, J. H. ADAIR and R. E. NEWNHAM, *ibid.* **25** (1990) 3634.
21. M. H. LEE, A. HALLIYAL and R. E. NEWNHAM, *J. Amer. Ceram. Soc.* **72** (1989) 986.
22. G. MARBACH, S. STOTZ, M. KLEE and J. W. C. DE VAIES, *Phys. C* **161** (1989) 111.
23. J. HAGBERG, R. RAUTIOAHO, J. LEVOSKA, A. UUSIMAKI, T. MURTONIEMI, T. KOKKMAKI and S. LEPPAVUORI, *ibid.* **160** (1989) 369.
24. A. SAFARI, Y. H. LEE, A. HALLIYAL and R. E. NEWNHAM, *Amer. Ceram. Soc.* **66** (1987) 668.
25. C. M. JIMENEZ, G. F. ARROYO and L. D. GUILLEN, in "Ceramic Powders," edited by P. Vincenzini (Elsevier Scientific Publishing, Amsterdam, 1983) p. 564.
26. C. LU and Y. XU, *Mater. Lett.* **27** (1996) 13.
27. M. GOBE, K. KON-NO, K. KANDORI and A. KITAHARA, *J. Coll. Interface Sci.* **93** (1983) 293.
28. S. HINGORANI, D. O. SHAH and M. S. MULTANI, *J. Mater. Res.* **10** (1995) 461.
29. K. KANDORI, K. KON-NO and A. KITAHARA, *J. Coll. Interface Sci.* **115** (1987) 579.
30. M. J. HOU and D. O. SHAH, in "Interfacial Phenomena in Biotechnology and Materials Processing," edited by Y. A. Attia, B. M. Moudgil and S. Chander (Elsevier, Amsterdam, 1988) pp. 443–458.
31. C. H. CHEW, L. M. GAN and D. O. SHAH, *J. Disp. Sci. Technol.* **11** (1990) 593.
32. P. AYYUB, A. N. MAITRA and D. O. SHAH, *Phys. C.* **168** (1990) 571.
33. P. AYYUB and M. S. MULTRANI, *Mater. Lett.* **10** (1991) 431.
34. G. K. LIM, J. WANG, S. C. NG and L. M. GAN, *ibid.* **28** (1996) 431.
35. L. M. GAN, H. S. O. CHAN, L. H. ZHANG, C. H. CHEW and B. H. LOO, *Mater. Chem. Phys.* **27** (1994) 263.
36. L. M. GAN, L. H. ZHANG, H. S. O. CHAN, C. H. CHEW and B. H. LOO, *J. Mater. Sci.* **31** (1996) 1071.
37. H. HERRIG and R. HEMPELMANN, *Mater. Lett.* **27** (1996) 287.
38. H. YAMAMURA, S. KURAMOTO, H. HANEDA, A. WATANABE and S. SHIRASAKI, *Yogyo, Kyokai Shi* **94** (1986) 470.
39. H. YAMAMURA, A. WATANABE, S. SHIRASAKI, Y. MORIYOSHI and M. TANADA, *Ceram. Int.* **11** (1985) 17.
40. J. FANG, J. WANG, S.-C. NG, C.-H. CHEW and L.-M. GAN, *Nanostruct. Mater.* **8** (1997) 499.
41. "Handbook of Inorganic Compounds," edited by D. L. Perry and S. L. Phillips (CRC Press, Boca Raton, 1995) p. 216.

Received 21 May 1997
and accepted 7 October 1998